Original

Yi, S.; Letzig, D.; Hantzsche, K.; Gonzalez Martinez, R.; Bohlen, J.;
Schestakow, I.; Zaefferer, S.:

Improvement of Magnesium Sheet Formability by Alloying Addition of Rare Earth Elements

In: Materials Science Forum, THERMEC 2009 (2010) Trans Tech Publications

DOI: 10.4028/www.scientific.net/MSF.638-642.1506

Materials Science Forum *Online: 2010-01-12*
ISSN: 1662-9752, Vols. 638-642, pp 1506-1511
doi:10.4028/www.scientific.net/MSF.638-642.1506

Improvement of magnesium sheet formability by alloying addition of rare earth elements

Sangbong Yi[1,a], Dietmar Letzig[1,b], Kerstin Hantzsche[1,c], Rodolfo Gonzalez Martinez[1,d], Jan Bohlen[1,e], Igor Schestakow[2,f] and Stefan Zaefferer[2,g]

[1]Magnesium Innovation Centre, GKSS Research Centre, Max-Planck-Strasse, D-21502, Geesthacht, Germany

[2]Max-Planck-Institute for Iron Research, Max-Planck-Strasse 1, D40237, Düsseldorf, Germany

[a]sangbong.yi@gkss.de, [b]dietmar.letzig@gkss.de, [c]kerstin.hantzsche@gkss.de, [d]rodolfo.gonzalez-martinez@gkss.de, [e]jan.bohlen@gkss.de, [f]i.schestakow@mpie.de, [g]s.zaefferer@mpie.de

Keywords: magnesium alloy, sheet rolling, formability, texture, microstructure

Abstract. The influences of rare earth elements addition on the crystallographic texture and microstructural evolutions are examined during rolling and annealing of Mg-sheets. In case of Nd or Y additions, dynamic recrystallisation is suppressed such that the deformed microstructure is observed after hot rolling with relatively large strain per pass. Cold rolled binary Mg-Nd alloy sheet shows strong texture with splitting of the basal poles in the rolling direction, however, the texture intensity decreases significantly during the recrystallisation annealing. From the comparison of deep drawing behaviours between commercial ZE10 and AZ31 sheets, it is observed that the addition of the rare earth elements and accompanying texture changes result in the improved formability.

Introduction

Poor formability of magnesium sheet, especially at room temperature, is one of the main reasons which retard industrial applications of this lightest structural metallic material. The strong basal-type texture formed through mechanical processing, such as sheet rolling, causes limited formability based on the restricted activities of the <a>-dislocations slip under loading in the sheet normal and planar directions. To overcome the above mentioned problems, it is necessary to provide a way of achieving weak texture and fine grained microstructure simultaneously during sheet rolling.

An effective way of altering the strong basal-type texture is to subject a large shear deformation to magnesium alloys, for example asymmetric rolling [1]. Another approach of the texture control is the addition of rare earth (RE) elements to magnesium alloys. Recently, it was reported that more randomized texture can be obtained through alloying additions of yttrium (Y) and RE elements such as neodymium (Nd) and cerium (Ce) [2,3]. Differently to the asymmetric rolling which leads to a shift of the basal texture component toward the rolling direction (RD), more randomized texture can be achieved by the RE elements addition.

The present study aims to investigate the influence of RE elements addition on the texture and microstructure evolution during rolling, subsequent annealing and forming processes. The Mg-Nd and Mg-Y binary alloys are chosen for tracking the effect of alloying elements on the microstructural evolution during warm rolling. To investigate the microstructural development during the deformation and recrystallisation separately, without the dynamic recrystallisation (DRX) which occurs unavoidably during hot rolling of Mg alloys, the cold rolling and recrystallisation annealing of the above alloys are carried out. The influence of modified texture and microstructure of the RE-alloyed Mg on the sheet formability is examined by deep drawing tests of rolled sheets of two commercial alloys. One is AZ31 alloy sheet which is representative for commercial Mg sheet alloys. The other is ZE10 containing a fair amount of Ce-misch metal, therefore, it can be considered as a representative for RE containing alloys.

Experimental procedures

Gravity casted Mg-1Nd, Mg-2Nd, Mg-1Y and Mg-3Y (in wt. %) alloys were machined to slabs for rolling. Hot rolling was conducted at 400°C using laboratory rolling mill to a total thickness reduction of 93 %, from 20 mm to 1.4 mm. The strain per pass was kept $\varphi = 0.2$ up to the thickness of about 1.9 mm. The last hot rolling step was, however, carried out with a strain value of $\varphi = 0.3$, i.e. 1.9 mm to 1.4 mm. After each pass, the sheets were intermediate annealed at 400°C for 20 min.

A strip was cut from the Mg-1Nd alloy after hot rolling to a thickness of 1.9 mm, and further rolled at room temperature. To avoid cracking, the thickness reduction per pass was controlled not to exceed 4% during the cold rolling ($\varphi < 0.05$ / pass) [4]. After 50% of the thickness reduction by cold rolling, i.e. at a final thickness of about 0.9 mm, the sheet was annealed at 350 °C for various times, 1 to 60 min.

Round blanks with the diameter of 85 mm were prepared for deep drawing experiments from the commercial AZ31 (Mg-2.8Al-0.8Zn–0.2Mn in wt. %) and ZE10 (Mg-1.3Zn-0.2Ce-0.1La) sheets with the thickness of 1.3 mm. Deep drawing experiments were carried out using an Erichsen universal sheet testing machine, with the drawing ratio, β=blank diameter/punch diameter, of 1.7 at different temperatures, 150, 200, 250 and 300°C. The punch speed and the blank holder force were kept constant for all test temperatures, 20 mm/min and 5 kN, respectively. The whole blank and the contact area of the punch were coated with boron nitride spay as lubricant.

Six incomplete pole figures of $\{10\bar{1}0\}$, (0002), $\{10\bar{1}1\}$, $\{10\bar{1}2\}$, $\{11\bar{2}0\}$ and $\{10\bar{1}3\}$ were measured by the X-ray diffraction (Pananlytical, 40 kV and 40 mA) for the global texture of the rolled sheets. The electron back scatter diffraction (EBSD) technique was applied to measure the microstructure of the rolled sheets as well as deep drawn cups. The samples for the EBSD measurements were taken from the longitudinal plane of the rolled sheets and the thickness plane along the RD of the drawn cups. The texture of the deep drawn cups will be presented only by using the EBSD results, because of the difficulties of the texture measurement of drawn cups using the conventional X-rays diffraction technique.

Results and Discussions

Hot rolling of binary alloys

The recalculated (0001) pole figures of hot rolled sheets are presented in Fig. 1. There is no significant difference between the hot rolled alloys in their texture types, in which the symmetrical splitting of the basal poles from ND toward RD are observed. The peak intensity of the (0001) pole figures are found at 13° ~ 15° from ND to RD. Moreover, the maximum intensities of the (0001) pole figures of Mg-Nd alloys are comparable to those of Mg-Y alloys.

This type of texture showing splitting of the basal pole into RD has been observed often in common AZ31 alloy sheets. Agnew et al. [5] reported that the activation of the <c+a> slip plays an important role for the formation of the texture with the tilted basal poles towards RD. Another mechanism of promoting the formation of the tilted basal pole is the activation of secondary twinning, in which $\{10\bar{1}1\}$ compression twinned area is re-twinned by $\{10\bar{1}2\}$ tensile system [6].

Fig. 2 shows the microstructure of the hot rolled Mg-1Y and Mg-2Nd alloys, in terms of the confidence index maps of EBSD measurements. The contrast values of the maps correspond to the indexing quality of the Kikuchi patterns of the EBSD measurements, and the non index-able area is presented with black color. Besides high angle grain boundaries (> 15°), the twin boundaries are marked with the following misorientation relations; 86° rotation around $<11\bar{2}0>$ for tensile twins, 56° around $<11\bar{2}0>$ for compression twins and 38° around $<11\bar{2}0>$ for secondary twins. Among three different twins marked in the Fig. 2 (a) and (b), the secondary twins are dominantly observed. Different to the microstructure of hot rolled AZ31 and AZ61 sheets which show large amount of the DRXed grains [7,8], the present results show clearly DRX is suppressed by addition of Nd and Y.

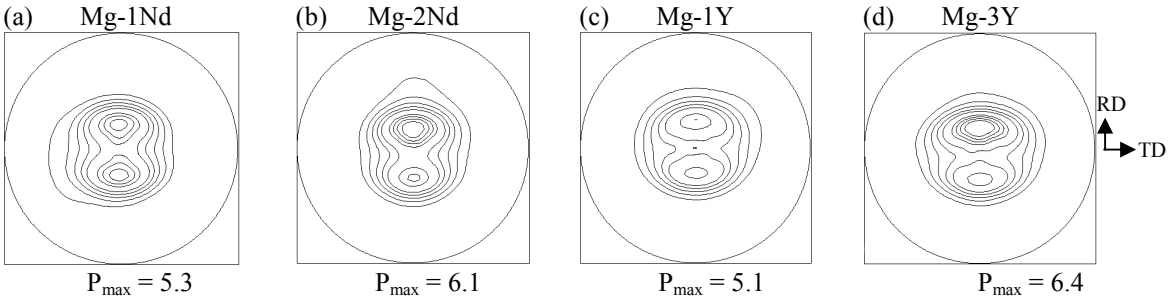

Fig.1 Recalculated pole figures of hot rolled sheets, (a) Mg-1Nd, (b) Mg-2Nd, (c) Mg-1Y and (d) Mg-3Y alloys (contours = 1, 1.5 … 5.5, TD: transverse direction, RD: rolling direction)

Consequently, a deformed microstructure is obtained after hot rolling under rolling conditions used in the present study. The non-indexed areas in the EBSD maps, marked with shadowed rectangles in Fig. 2, correspond to shear bands, which align with rotation of about 30° from RD. These bands are also visible in optical micrographs (not shown). Interestingly, the traces of the secondary twins are found at the end (or beginning) of the shear bands. Moreover, secondary twinning boundaries are visible at the mid-position of some shear bands.

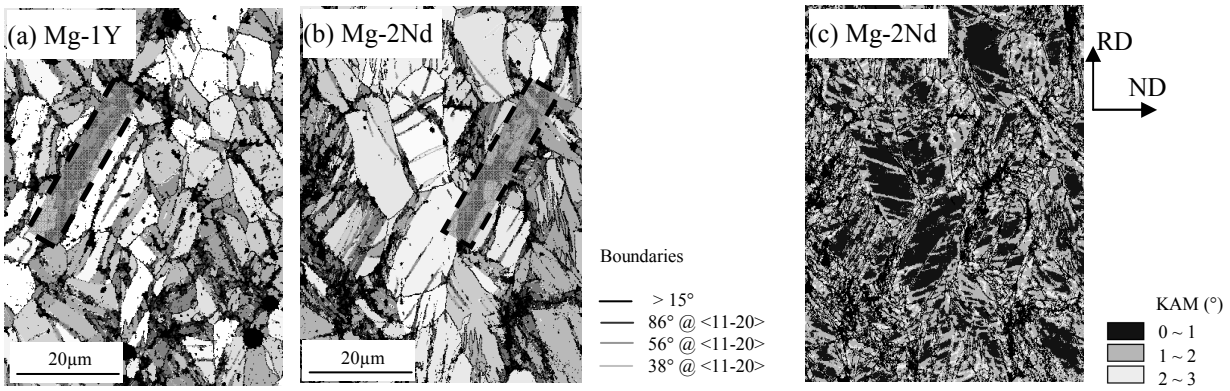

Fig. 2 EBSD confidence index maps of hot rolled (a) Mg-1Y and (b) Mg-2Nd sheets. (c) Kernel average misorientation map of Mg-2Nd alloy, same area with (b).

These observations indicate that shear band formation initiates at the secondary twins. Since the orientation of the secondary twins are fairly advantageous for activation of <a>-type dislocations, it is expected that localized deformation occurs at secondary twins. A kernel average misorientation (KAM) map of Mg-2Nd alloy is shown in Fig. 2 (c). The KAM map represents the local misorientation and the degree of the strain energy on a grain level. This map is constructed based on the misorientation degree between a measuring point (so called, kernel) and its all neighbours at the periphery. The KAM map confirms the localised deformation around twinned areas, such that relative high KAM values are observed along the twins.

Cold rolling and static recrystallisation

The microstructure variation during the annealing at 350 °C of the 50 % cold rolled Mg-1Nd alloy is shown in Fig. 3, in terms of the inverse pole figure maps in ND. It is worthwhile to repeat that the sheet used for the cold rolling received a final rolling pass with $\varphi = 0.2$ which is lower compared to the above presented sheets in Fig. 2. For this reason, it contains many secondary twins, but, no shear bands. The shear bands shown in the Fig. 3 (a) are formed during cold rolling, and they align at about 30° rotated from RD.

Fig. 3 (b) presents the microstructure after 3 min annealing at 350 °C. As marked with shadowed rectangle in the figure, the agglomerates of the small grains are found along the former shear bands.

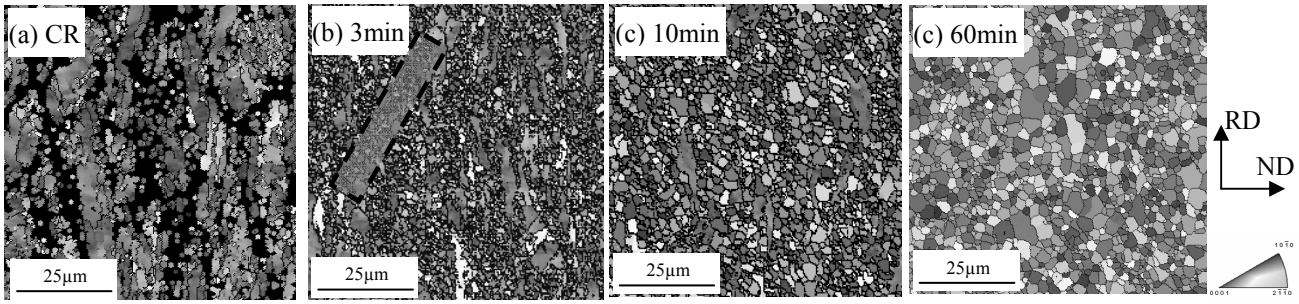

Fig. 3 Microstructure of Mg-1Nd alloy, in terms of the EBSD inverse pole figure maps in ND, after (a) 50% cold rolling and annealing at 350°C for (b) 3 min, (c) 10min and (d) 60 min. The dotted circles marked in (c) indicate the non-recrystallised structure.

That is, the shear bands act as the beginning sites of the recrystallisation. The texture of the recrystallised grains is weaker than the non-recrystallised grains, which can be also seen indirectly by the various colors of the small grains in Fig 3 (b) and (c). With increasing the annealing time, the new grains formed at the shear band grow and consume the deformed grains. After full consumption of the deformed grains, e.g. after annealing for 60 min shown in Fig. 3 (d), a microstructure comprised of fine equi-axed grains is obtained (average grain size = 8 μm).
The recalculated (0001) pole figures of the cold rolled and annealed samples are illustrated in Fig. 4. The strong texture of the cold rolled sheet with the basal pole tilted about 13° in RD becomes rapidly weak with increasing the annealing time. The maximal intensity of the (0001) pole figure decreases from P_{max} = 7.4 m.r.d. (multiple random degree) of the cold rolled sheet to P_{max} = 3.9 m.r.d. after 60 min annealing at 350 °C. As shown in Fig. 3 and Fig. 4 (b), the texture weakening occurs mainly during the growth of newly recrystallised grains. In addition, the increase of the angular distance between two basal poles with peak intensity is observed, Fig. 4 (c).

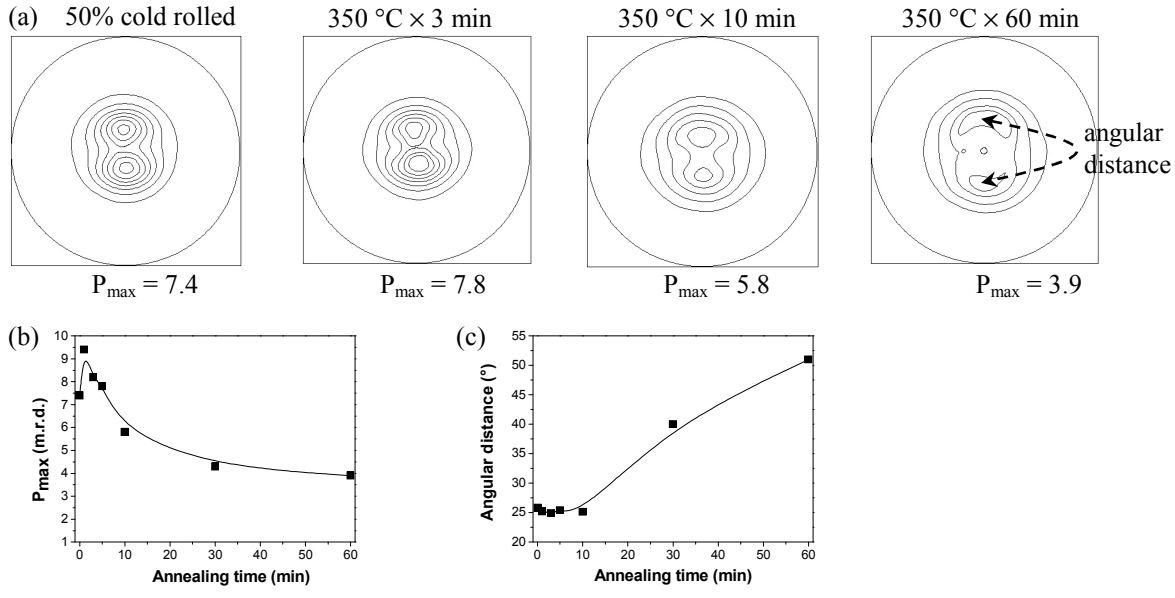

Fig. 4 (a) Recalculated (0001) pole figures of 50% cold rolled and after annealing at 350°C for various time (contours = 1, 2 … 7). (b) Variation of the maximal intensity of (0001) pole figures and (c) the angular distance of the two basal poles corresponding to the peak intensity during annealing at 350 °C.

Deep drawing of AZ31 and ZE10 sheets

The results from the cup drawing tests conducted using commercial AZ31 and ZE10 sheets are summarized in Fig. 5. The AZ31 sheet should be heated up to 200°C for successful forming, while

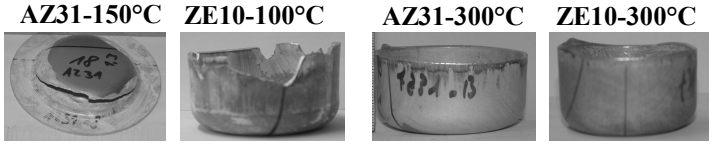

	Deep drawing temperature (°C), β = 1.7				
	100	150	200	250	300
AZ31	F	F	G	G	G
ZE10	F	G	G	G	G

Fig. 5 AZ31 and ZE10 cups formed at different temperatures. The table on the right side lists the drawability as a function of the working temperature (G: successful, F: failed).

the ZE10 sheet can be drawn successfully at 150 °C.

Fig. 6 shows the microstructure of AZ31 and ZE10 cups drawn at 300 °C. The microstructure and the texture of the initial sheets can be referred to those measured at the bottom of the drawn cups, Fig. 6 (b) and Fig. 7 (b). The bottom parts experienced almost ignorable deformation during the deep drawing. Moreover, the bottom parts were kept at near room temperature because of the direct contact with the unheated punch, while the wall parts were heated constantly at the drawing temperature. Contrary to the bottom, remarkable changes in microstructures as well as texture are observed at the wall of the drawn cups. DRXed fine grains are observed in the AZ31 alloy, which align along the lines tilted about 30° from the drawing direction (x), marked as dashed lines in Fig. 6 (a). The ZE10 alloy shows elongated grains in the drawing direction without DRX. Most grains have large internal orientation gradient and fragmentation into small domains with low misorientation (< 5°), marked as dashed circles in Fig. 6 (a). Above difference in DRX behaviors between AZ31 and ZE10 alloys can be explained by following two factors; firstly, the relatively weak main texture component of ZE10 sheet corresponds to the basal planes tilted 30~40° from the sheet normal direction. Thus, it is favorable for the <a> dislocations slip such that the strain can be accommodated relatively easily by dislocation glide. Differently to ZE10, the texture of the AZ31 sheet is unfavorable for the <a> slip. It can be expected, therefore, that the strain is accommodated in AZ31 alloy by another deformation mechanism, e.g. <c+a> slip and / or formation of shear zones in the regime of DRX as shown in Fig. 6. Secondly, the existence of the heavy RE-elements in the ZE10 alloy, in form of solid solution and precipitates, can retard the DRX process, by solute drag or boundary pinning.

Fig. 7 presents the $\{10\bar{1}0\}$ and (0001) pole figures calculated using the EBSD data. The texture of the AZ31 alloy at the wall shows an isotropic distribution of the c-axes around the thickness direction, which is different to the initial sheet texture having oval-shaped distribution with its long axis in RD. Though the mechanism leading to the formation of the sharp basal texture during deep

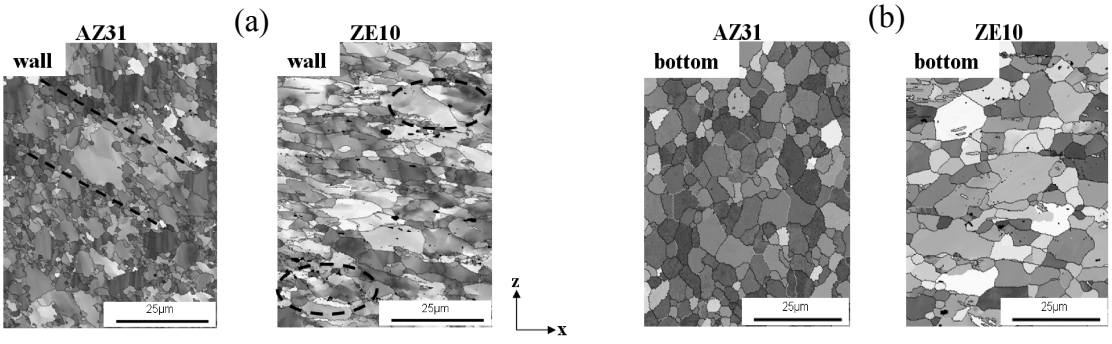

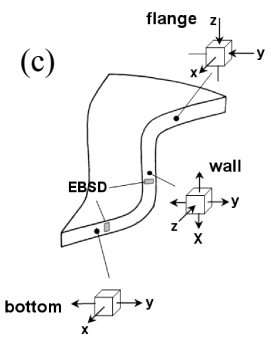

Fig. 6 Orientation maps measured (a) at the wall and (b) the bottom of AZ31 and ZE10 cups formed at 300 °C. (c) Schematics showing the strain-state, sample coordinate during deep drawing and the positions of EBSD measurements.

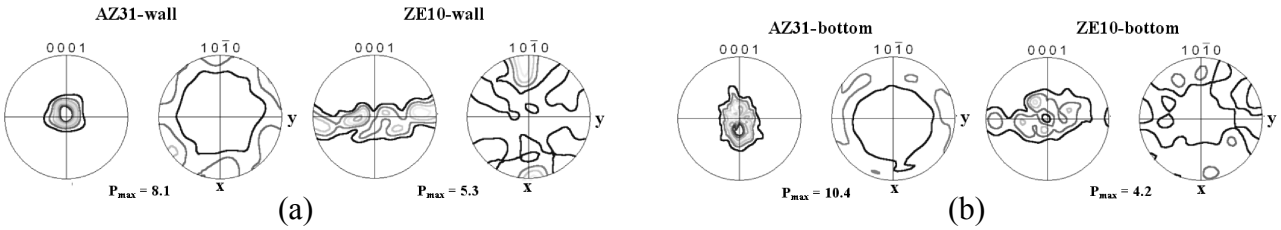

Fig. 7 (0001) and $\{10\bar{1}0\}$ pole figures of deep drawn cups calculated using the EBSD data: (a) at the wall and (b) bottom.

drawing process is not yet understood, we believe that the DRX at high strain rate leads to the formation of this texture type. Based on this texture change to the symmetric shape, the drawn cup does not show earing behavior, *see* AZ31 cup drawn at 300°C in Fig. 5. Comparing the texture of the ZE10 initial sheet to the drawn cup, the strengthening of the component having the c-axes parallel to the radial direction is obvious. Moreover, the strengthening of $<10\bar{1}0>$ component parallel to the drawing direction, former RD, is also observed. Since the ZE10 alloy is deformed without thermally activated mechanism like DRX, the planar anisotropy observed in the initial sheet appears as earing phenomena, *see* ZE10 cup drawn at 300°C in Fig. 5.

Summary

The deformation during the hot rolling with relatively large strain per pass and the cold rolling is accommodated by the shear bands which are initiated mainly at the secondary twins. The recrystallisation begins at the shear bands during the annealing of the cold rolled Mg-1Nd sheet. The significant weakening of the global texture during the annealing is accompanied mainly with the grain growth. The weak texture in the commercial ZE10 sheet contributes to the improved sheet formability, which was examined by cup drawing in the present study, and to the suppressed DRX.

Acknowledgements

It is gratefully acknowledged that the present study is supported by DFG (under grant YI103/1-1 and ZA278/6-1). Authors appreciate the deep drawing experiments of F. Heinemann and the technical supports of V. Kree in GKSS research centre with microstructure analyses.

References

[1] W.J. Kim, J.B. Lee, W.Y. Kim, H.T. Jeong and H.G. Jeong: Scripta Mater. Vol. 54 (2007), p. 309.

[2] J. Bohlen, M.R. Nürnberg, J.W. Senn, D. Letzig and S.R. Agnew: Acta Mater. Vol. 55 (2007), p. 2101.

[3] J. Wendt, K.U. Kainer, G. Arruebarrena, K. Hantzsche, J. Bohlen and D. Letzig, in: *Magnesium Technology 2009*, edited by E. Nyberg, S. Agnew and O. Pekguleyuz (TMS, 2009)

[4] S.L. Couling, J.F. Pashak and L. Sturkey: Tans. ASM Vol. 51 (1958), p. 94.

[5] S.R. Agnew, M.H. Yoo, C.N. Tomé: Acta Mater. Vol. 49 (2001), p. 4277.

[6] B.C. Wonsiewicz and W.A. Backofen: Tans. Metall. Soc. AIME Vol. 239 (1966), p. 1422.

[7] M.T. Pérez-Prado, J.A. del Valle, J.M. Contreras and O.A. Runao: Scripta Mater. Vol. 50 (2004), p. 661.

[8] H.T. Jeong and T.K. Ha: Mater. Proc. Tech. Vol.187-188 (2007), p. 559.